

Integrated design of Smart Structures

Original

Integrated design of Smart Structures / Cimellaro, G.P., Soong, T.T., Reinhorn, A.M.. - ELETTRONICO. - 56:(2008), pp. 127-136. (CIMTEC 2008 - Proceedings of the 3rd International Conference on Smart Materials, Structures and Systems - Embodying Intelligence in Structures and Integrated Systems Acireale, Sicily, Italy 8-13, June).

Availability:

This version is available at: 11583/1898355 since: 2016-11-18T13:21:07Z

Publisher:

Trans Tech Publications Ltd.

Published

DOI:

Terms of use:

This article is made available under terms and conditions as specified in the corresponding bibliographic description in the repository

Publisher copyright

(Article begins on next page)

Integrated Design of Smart Structures

G.P. Cimellaro^{1,a}, T. T. Soong^{2,b} and A.M. Reinhorn^{3,c}

¹Postdoctoral Research Associate, Department of Civil, Structural & Environmental Engineering, University at Buffalo, The State University of New York. 206 Ketter Hall, Buffalo, NY 14260, U.S.A.

²SUNY Distinguished Professor and Samuel P. Capen Professor of Engineering Science, Department of Civil, Structural & Environmental Engineering, University at Buffalo, The State University of New York. 238 Ketter Hall, Buffalo, NY 14260, U.S.A.

³Clifford C Furnas Eminent Professor, Department of Civil, Structural & Environmental Engineering, University at Buffalo, The State University of New York. 135 Ketter Hall, Buffalo, NY 14260, U.S.A.

^agpc2@buffalo.edu, ^btsoong@buffalo.edu, ^creinhorn@buffalo.edu

Keywords: structural control, integrated design, structural optimization.

Abstract. Much of structural control research and applications in civil engineering have been concerned with structures equipped with passive, hybrid, or active control devices in order to enhance structural performance under extraordinary loads. In most cases, the structure and the control system are individually designed and optimized. On the other hand, an exciting consequence of structural control research is that it also opens the door to new possibilities in structural forms and configurations, such as lighter buildings or bridges with longer spans without compromising on structural performance. Moreover, this can only be achieved through integrated design of structures with control elements as an integral part. This paper addresses the integrated design of structures with imbedded control systems and devices. Simultaneous optimization of such controlled structures is considered, showing that new structural forms and configurations can be achieved through integrated design.

Introduction

In recent years, several approaches have been proposed for integrated design of structure/control systems in aerospace and civil engineering structures. For civil engineering structures, for example, a variational approach has produced good results [1-2]. However, due to complex nature of the resulting equations, the optimization problem is usually nonconvex. Therefore, numerical techniques are usually required to obtain a solution.

Redesign approach

The optimization problem becomes easier when the design procedure is divided in two steps. In fact, in control of buildings, the structure is traditionally designed first and then the controller. The proposed method reverses the procedure by designing the structure after the controller is given. The fundamental idea of redesign was proposed by Smith *et al.* [3]. In this section, the idea of redesign is incorporated into the integrated design of civil engineering structural/control systems. The procedure is summarized in the following steps:

First Step. The desired structure is chosen and it is assumed fixed while the controller is designed in order to satisfy a given performance requirement (e.g., drift, absolute acceleration, base shear, etc.) of the initial structure. The dynamic response of the initial structure in this step is called "Target Response".

Second Step. The structure and the controller are designed co-operatively to achieve a common goal (the Target dynamic response of the first step). This structure redesign is accomplished to reduce (minimize) the amount of active control power needed to achieve the “Target Response”. In other words, the structure is redesigned for better controllability. These two steps can be better understood by considering relationship between spectral acceleration and spectral displacement (S_a - S_d) in structural design. In Figure 1 is shown a typical (S_a - S_d) spectrum for several damping levels. $S_d(T_0, \beta_0)$ and $S_a(T_0, \beta_0)$ are the spectral coordinates of the original structure with period T_0 and damping β_0 . In *Step 1*, the structure at point 1 is made lighter by reducing its stiffness and it moves to point 2 in Figure 1. Then a controller is applied to bring back the structure to the initial Target response at point 3. In *Step 2*, the structure is redesigned in order to achieve the same performance, but with less amount of active control forces or damping. During the redesign, mass, stiffness and damping are modified in order to achieve this goal, reaching finally point 4 in Figure 1. At the end of this step, the building will maintain the same performance, but with less amount of control forces. The integrated redesign procedure is formulated in the following, for the case when the building is assumed linear for simplicity.

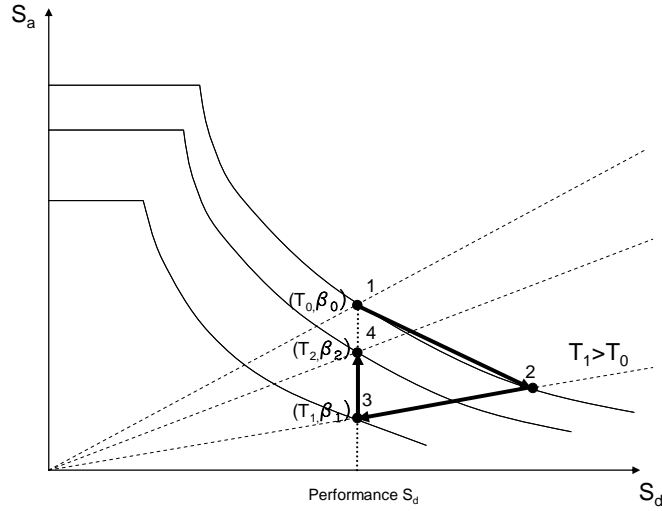


Figure 1 Redesign procedure in S_d - S_a plane

Following Smith *et al.* [3] consider a multi-degree-of-freedom linear building structure subjected to an external excitation. The equation of motion with active control force is given by

$$\mathbf{M}\ddot{\mathbf{x}}(t) + \mathbf{C}\dot{\mathbf{x}}(t) + \mathbf{K}\mathbf{x}(t) = \mathbf{H}\mathbf{u}(t) + \boldsymbol{\eta}w(t). \quad (1)$$

where $\mathbf{x}(t)$ is the displacement vector, \mathbf{M} , \mathbf{C} and \mathbf{K} are, respectively, the mass, inherent damping and stiffness matrices; $\mathbf{u}(t)$ is the active control force vector; \mathbf{H} is the location matrix for the active control forces; $\boldsymbol{\eta}$ is the excitation influence matrix; \mathbf{T}_s is the location matrix of the restoring forces and $w(t)$ is the external excitation. In the state space, Equation (1) becomes:

$$\dot{\mathbf{z}}(t) = \mathbf{A}\mathbf{z}(t) + \mathbf{B}\mathbf{u}(t) + \mathbf{e}(t). \quad (2)$$

where

$$\mathbf{z}(t) = \begin{bmatrix} \mathbf{x}(t) \\ \dot{\mathbf{x}}(t) \end{bmatrix}, \quad \mathbf{e}(t) = \begin{bmatrix} \mathbf{0} \\ \mathbf{M}^{-1}\boldsymbol{\eta} \end{bmatrix} w(t), \quad \mathbf{A} = \begin{bmatrix} \mathbf{0} & \mathbf{I} \\ -\mathbf{M}^{-1}\mathbf{K} & -\mathbf{M}^{-1}\mathbf{C} \end{bmatrix}, \quad \mathbf{B} = \begin{bmatrix} \mathbf{0} \\ \mathbf{M}^{-1}\mathbf{H} \end{bmatrix}. \quad (3)$$

Step 1. A control law is employed such that the structural system has acceptable performance such as satisfaction of certain constraints on the dynamic response. Many methods are available. Using a linear control law, for example $\mathbf{u}(t)$ can be expressed as

$$\mathbf{u}(t) = \mathbf{G}\mathbf{z}(t). \quad (4)$$

where \mathbf{G} is the gain matrix.

Step 2. Following *Step 1*, the redesign concept is to change the mass, stiffness, damping matrices, respectively, by $\Delta\mathbf{M}$, $\Delta\mathbf{K}$ and $\Delta\mathbf{C}$, and to determine the control force \mathbf{u} so that the new system becomes

$$(\mathbf{M} + \Delta\mathbf{M})\ddot{\mathbf{x}}(t) + (\mathbf{C} + \Delta\mathbf{C})\dot{\mathbf{x}}(t) + (\mathbf{K} + \Delta\mathbf{K})\mathbf{x}(t) = \mathbf{H}\mathbf{u}_a(t) + \boldsymbol{\eta}w(t). \quad (5)$$

where

$$\mathbf{u}_a(t) = \mathbf{G}_a\mathbf{z}(t). \quad (6)$$

where \mathbf{G}_a is the active part of the controller after redesign. The main idea is to separate the control law, Equation (4), into a passive part which is implemented into the physical system by redesign, and an active part which constitutes the remaining active control law required after structure redesign. Therefore, the control law is written in the following form

$$\mathbf{H}\mathbf{u}(t) = \mathbf{H}\mathbf{G}\mathbf{z}(t) = \mathbf{H}\mathbf{G}_a \begin{bmatrix} \mathbf{x}(t) \\ \dot{\mathbf{x}}(t) \end{bmatrix} - \Delta\mathbf{M}\ddot{\mathbf{x}}(t) - \Delta\mathbf{C}\dot{\mathbf{x}}(t) - \Delta\mathbf{K}\mathbf{x}(t). \quad (7)$$

and the closed-loop system after redesign is

$$(\mathbf{M} + \Delta\mathbf{M})\ddot{\mathbf{x}}(t) + (\mathbf{C} + \Delta\mathbf{C})\dot{\mathbf{x}}(t) + (\mathbf{K} + \Delta\mathbf{K})\mathbf{x}(t) = \mathbf{H}\mathbf{G}_a\mathbf{z}(t) + \boldsymbol{\eta}w(t). \quad (8)$$

where $\mathbf{u}_a(t)$, which is given by the Equation (6), is the active part of the controller and $\Delta\mathbf{M}\ddot{\mathbf{x}}(t) + \Delta\mathbf{C}\dot{\mathbf{x}}(t) + \Delta\mathbf{K}\mathbf{x}(t)$ is the passive part. The objective of the redesign is to find the passive control ($\Delta\mathbf{M}$, $\Delta\mathbf{K}$, $\Delta\mathbf{C}$) in order to minimize the control power needed to satisfy Equation (7) for any given \mathbf{G} . Note that the closed-loop system response before and after redesign remains unchanged; therefore, all the designed closed-loop system properties remain unchanged.

Let \mathbf{B}_k , \mathbf{B}_c and \mathbf{B}_m be the stiffness, damping and mass connectivity matrices of the structural system. The changes in the structural parameters can be expressed in the form

$$\begin{aligned} \Delta\mathbf{K} &= \mathbf{B}_k \mathbf{G}_k \mathbf{B}_k^T \\ \Delta\mathbf{C} &= \mathbf{B}_c \mathbf{G}_c \mathbf{B}_c^T \\ \Delta\mathbf{M} &= \mathbf{B}_m \mathbf{G}_m \mathbf{B}_m^T \end{aligned} \quad (9)$$

where

$$\begin{aligned}
\mathbf{G}_k &= \text{diag}(\dots, \Delta k_i, \dots) \\
\mathbf{G}_c &= \text{diag}(\dots, \Delta c_i, \dots) \\
\mathbf{G}_m &= \text{diag}(\dots, \Delta m_i, \dots)
\end{aligned} \tag{10}$$

This gives the following presentation for the desired control law

$$\mathbf{H}\mathbf{G} \begin{bmatrix} \mathbf{x}(t) \\ \dot{\mathbf{x}}(t) \end{bmatrix} = \mathbf{H}\mathbf{G}_a \begin{bmatrix} \mathbf{x}(t) \\ \dot{\mathbf{x}}(t) \end{bmatrix} - [\Delta\mathbf{K} \quad \Delta\mathbf{C}] \begin{bmatrix} \mathbf{x}(t) \\ \dot{\mathbf{x}}(t) \end{bmatrix} - \Delta\mathbf{M}\ddot{\mathbf{x}}(t). \tag{11}$$

Substituting the solution of $\ddot{\mathbf{x}}(t)$ from Equation (1), it yields

$$\mathbf{H}\mathbf{G}\mathbf{z}(t) = \mathbf{H}(\mathbf{G}_{active} + \mathbf{G}_{passive})\mathbf{z}(t). \tag{12}$$

where

$$\mathbf{G}_{active} = \mathbf{G}_a. \tag{13}$$

$$\mathbf{G}_{passive} = -\mathbf{I}_0\mathbf{B}_p\mathbf{G}_p\mathbf{B}_p^T\mathbf{L}. \tag{14}$$

with

$$\mathbf{B}_p = \begin{bmatrix} B_k & 0 & 0 \\ 0 & B_c & 0 \\ 0 & 0 & B_m \end{bmatrix}, \mathbf{G}_p = \begin{bmatrix} G_k & 0 & 0 \\ 0 & G_c & 0 \\ 0 & 0 & G_m \end{bmatrix}, \mathbf{I}_0 = [I \quad I \quad I], \mathbf{L} = \begin{bmatrix} I \\ \mathbf{M}^{-1}(\mathbf{H}\mathbf{G} - [\mathbf{K} \quad \mathbf{C}]) \end{bmatrix} \tag{15}$$

An approach to solving numerically the constrained optimization problem is to use the “*Exterior penalty function method*” that is part of the Sequential Unconstrained Minimization Techniques (SUMT), because it requires the solution of several unconstrained minimization problems.

Numerical examples

SDOF steel portal frame.

Consider a 2-D moment resisting one-story and one-bay steel frame (Figure 2). The frame consists of two columns (W14×257 and W14×311) and one beam (W33×118). The columns are 345 MPA (50ksi) steel and the beam is 248 MPA (36ksi). The bay width L is 9.15m (30ft) and the height h is 3.96m (13 ft). The frame is subjected to a zero-mean white noise stationary horizontal base acceleration with peak ground acceleration of 0.25 g. The mass is $M=159.450 \text{ kN sec}^2/\text{m}$, the stiffness is $K=76987.117 \text{ kN/m}$ and the damping coefficient is $C= 140.147 \text{ kN sec/m}$ that is determined assuming Rayleigh damping equal to 2%.

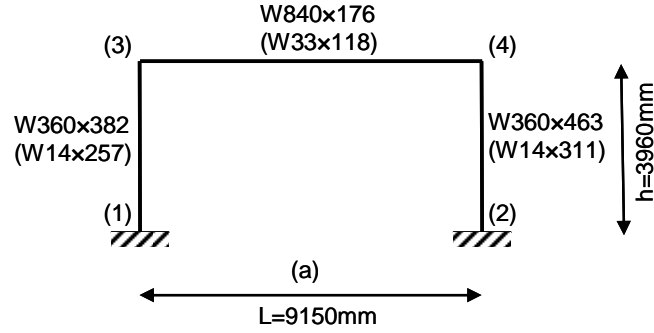


Figure 2. SDOF steel frame under white noise excitation

The period of the uncontrolled frame is $T_0 = 0.28$ sec. The required lateral stiffness K_s necessary for supporting the gravity loads is

$$K_s = 0.18K . \quad (16)$$

The frame has been designed in order to limit the drift to 0.5% ($x_{lim} = 1.98$ cm). Following *Step 1*, consider now a possible reduction of K by introducing a diagonal active brace member while maintaining the original performance level (0.5% drift). Mass will be changed accordingly while damping reduces according to Rayleigh damping constraint. For the active structure, the equation of motion can be written as

$$M_a \ddot{x}(t) + C_a \dot{x}(t) + K_a x(t) = Hu(t) + \eta w(t) . \quad (17)$$

where K_a is the achievable stiffness in the columns of the active structure and $u(t)$ is the control force in the active brace, which can be determined by using a control algorithm such as LQR. Figure 3 shows the value of K_a as a function of the achievable maximum displacement and the corresponding required maximum control force u_{MAX} . In particular, it is possible to choose K_a while the dynamic requirements are satisfied entirely through activation of the active brace. In this example, a reduction of stiffness of 60% is selected in order to satisfy the same performance level of 0.5% drift with a maximum active control force of 94.86 kN (Figure 3b).

Many combinations are possible in determining the section properties of the columns and the beam for which it is possible to obtain a stiffness reduction of about 60%. In this example, the two columns are substituted by two W14x99 sections. Using this selection, it is possible to obtain a reduction of stiffness of 61.8% and the new updated stiffness is

$$K_a = 29401.127 \text{ kN/m} . \quad (18)$$

The initial structural steel mass of the frame is

$$M_{s0} = 10924 \text{ lb} = 4959.5 \text{ kg} . \quad (19)$$

With added active brace, the structural steel mass is

$$M_s = 6114 \text{ lb} = 2775.7 \text{ kg} . \quad (20)$$

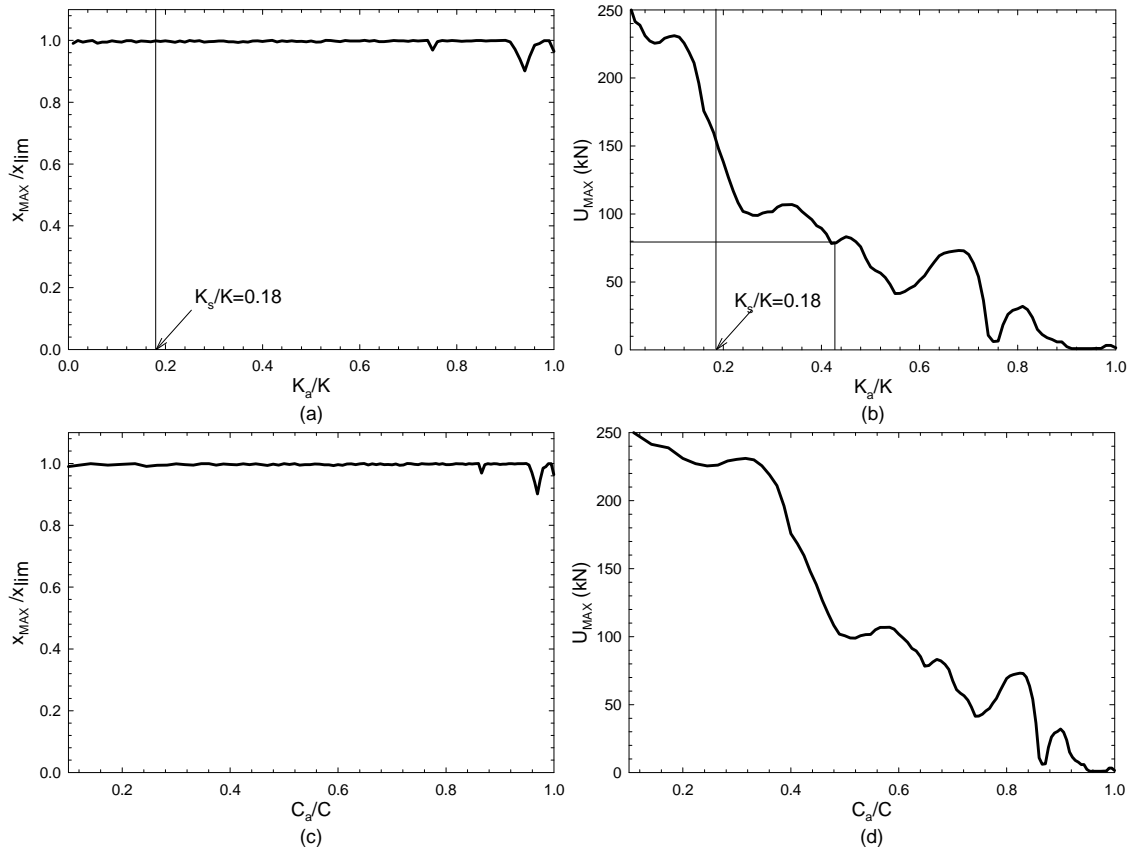


Figure 3. Normalized maximum displacement (a) and maximum control force (b) versus normalized structural stiffness and damping (c-d)

Consequently, the structural steel weight is reduced by 44% by adding an active brace with a maximum control force of 94.86 kN. Table 1 gives the maximum drift and absolute acceleration response for the initial structure and the redesigned structure with the active brace installed. Table 1 also shows that it is possible to obtain a reduction of structural steel mass without modifying the performance of the structure.

Table 1 Maximum response for white noise with pga of 0.25g

Uncontrolled			$U_{max}=94.86\text{kN}$		
(1)	(2)	(3)	(4)	(5)	(6)
Drift x_i [%]	\ddot{x}_a [m/sec ²]	M_{S0} [kg]	Drift x_i [%]	\ddot{x}_a [m/sec ²]	M_S [kg]
0.49	11.15	4959.5	0.50	5.81	2775.7

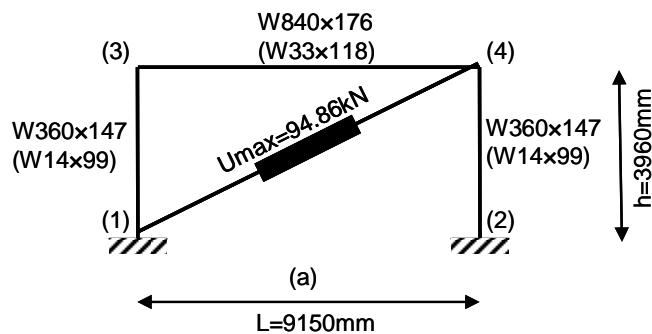


Figure 4 Steel portal frame with active brace

Step 2 of the redesign procedure can now be carried out by minimizing control power while keeping drift at 0.5%. By imposing a lower bound for the lateral stiffness equal to K_s in Equation (16) and assuming a lower bound for the mass at 75% of the initial value, the optimal structural parameters and the associated control force are given in Table 2. The percentage reduction of mass is -25%, stiffness is -62.3% and damping is -39.5%.

Table 2 Optimal structural parameters after redesign for white noise with pga of 0.25g

M	K	C	
kg	kN/m	kN sec/m	
159450	76987.1	140.1	

M_{opt}	K_{opt}	C_{opt}	U_{opt}
kg	kN/m	kN sec/m	kN
119587	29010.1	59.930	92.434

It is shown that a substantially lighter structure can be designed to achieve a specified performance objective when an active brace is integrated into the structure in an optimal fashion.

MDOF 9-story shear-type building.

The nine-story benchmark structure [4] considered in this example is 45.73 m (150 ft) by 45.73 m (150 ft) in plan, and 37.19 m (122 ft) in elevation. The bays are 9.15 m (30 ft) on center, in both directions, with five bays each in the North-South (N-S) and East-West (E-W) directions. The building's lateral load-resisting system is comprised of steel perimeter moment-resisting frames (MRFs) with simple framing on the furthest south E-W frame. The interior bays of the structure contain simple framing with composite floors. Typical floor-to-floor heights (measured from center-of-beam to center-of-beam for analysis purposes) are 3.96 m (13 ft). The floor-to-floor height of the basement level is 3.65 m (12 ft) and for the first floor is 5.49 m (18 ft).

Table 3. Drift and Acceleration response during Step 1 of the algorithm

Story level	Target Response		$T^*_1/T_1=1.831$		Active LQR		
	(1)	(2)	(3)	(4)	(5)	(6)	(7)
No.	Drift [%]	\ddot{x}_a [m/sec ²]	Drift [%]	\ddot{x}_a [m/sec ²]	Drift [%]	\ddot{x}_a [m/sec ²]	U_{max} [kN]
9	0.31	3.61	0.80	3.09	0.31	2.03	173.39
8	0.18	2.97	0.47	2.64	0.15	1.85	159.72
7	0.94	2.71	2.55	2.46	0.77	1.77	153.86
6	0.27	2.71	0.76	2.86	0.22	1.87	163.49
5	0.90	2.64	2.74	2.99	0.86	1.88	165.26
4	0.42	3.74	1.39	2.64	0.43	2.04	151.52
3	0.38	3.50	1.04	2.67	0.37	2.10	127.90
2	0.38	2.95	0.92	2.62	0.38	1.99	97.91
1	0.79	2.79	1.87	2.47	0.76	1.98	66.67

1: The stiffness is reduced proportionally to 30% of the initial lateral stiffness

The floor system is comprised of 248 MPa (36 ksi) steel wide-flange beams acting compositely with the floor slab, each frame resisting one-half of the seismic mass associated with the entire structure. The seismic mass at the ground level is 9.65×10^5 kg (66.0 kip-sec²/ft), 1.01×10^6 kg (69.0 kips-sec²/ft) for the first level, 9.89×10^5 kg (67.7 kip-sec²/ft) for the second through eighth

levels and 1.07×10^6 kg (73.2 kip-sec²/ft) for the ninth level. The seismic mass of the above ground levels of the entire structure is 9.00×10^6 kg (616 kip-sec²/ft). More details about the model can be found in Othori *et al.* [4]. A shear type model has been developed with the information available. The stiffness values are reported in column 4 of Table 5, while the first three frequencies of the model are 0.45, 1.28 and 1.99 Hz. Rayleigh proportional damping is considered, including 2% of damping ratio for the first two modes. The structure is subjected to the first 30 sec of white noise with amplitude of 0.15g and with a sampling frequency of 0.02 sec.

Table 4. Drift and acceleration response for the redesign structure

Story level	Uncontrolled		Redesign approach		
(1)	(2)	(3)	(4)	(5)	(6)
No.	Drift [%]	\ddot{x}_a [m/sec ²]	Drift [%]	\ddot{x}_a [m/sec ²]	Umax [kN]
9	0.31	3.61	0.23	1.87	134.97
8	0.18	2.97	0.10	1.67	107.11
7	0.94	2.71	0.67	1.89	110.81
6	0.27	2.71	0.19	1.70	114.80
5	0.90	2.64	0.73	1.80	125.26
4	0.42	3.74	0.34	1.90	113.00
3	0.38	3.50	0.31	1.98	113.42
2	0.38	2.95	0.31	1.96	108.17
1	0.79	2.79	0.71	1.93	57.02

In Table 3 are shown the drift and acceleration response during *Step 1* of the algorithm. In column 2 and 3 are shown the drift and the acceleration response of the initial building or, in other words, the performance requirement to be achieved (*Target Response*).

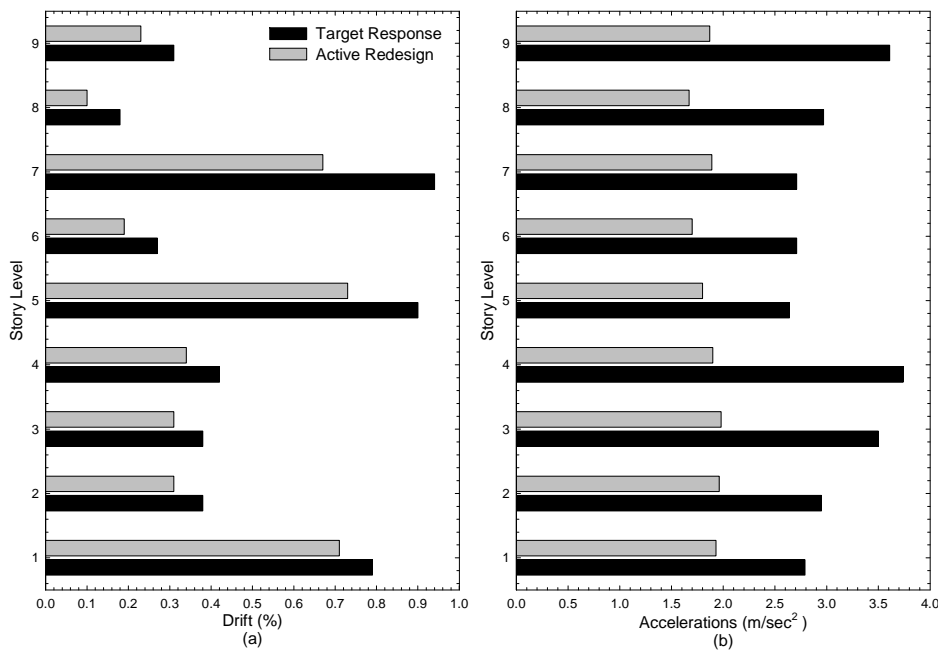


Figure 5 Response comparison with Redesign approach

Initially, the story lateral stiffness is reduced proportionally to 30% of the initial stiffness value in order to obtain a first natural period increment of 83%. Response of the lightweight structure is shown in columns 4 and 5 of Table 3.

Then, an active brace is applied at each story level in order to achieve the same performance in term of drift of the uncontrolled initial structure.

Table 5. Optimal structural parameters after redesign using a white noise with pga of 0.15 g

Story level	M	C	K	Mopt	Copt	Kopt
(1)	(2)	(3)	(4)	(5)	(6)	(7)
	kN sec ² /m	kN sec/m	103 kN/m	kN sec ² /m	kN sec/m	10 ³ kN/m
9	534.1	411.4	100.02	350.3	1352.5	18.21
8	494.7	1152.8	291.12	342.2	5843.8	62.79
7	494.7	390.9	71.52	336.0	434.9	15.68
6	494.7	1077.4	247.63	348.3	2284.2	56.02
5	494.7	487.5	75.03	361.2	289.9	16.89
4	494.7	877.3	170.08	370.0	596.6	39.98
3	494.7	1119.4	224.76	423.7	984.1	54.02
2	494.7	1301.4	263.02	474.1	1841.0	65.92
1	503.5	906.5	143.48	441.3	723.7	36.21

Values of the maximum active control force at each story level are shown in column 8 of Table 3. The coefficient p [5] of the R matrix, it is assumed equal to 11.6 to obtain a maximum drift below 1.0% when excited with a white noise of 0.15g of amplitude.

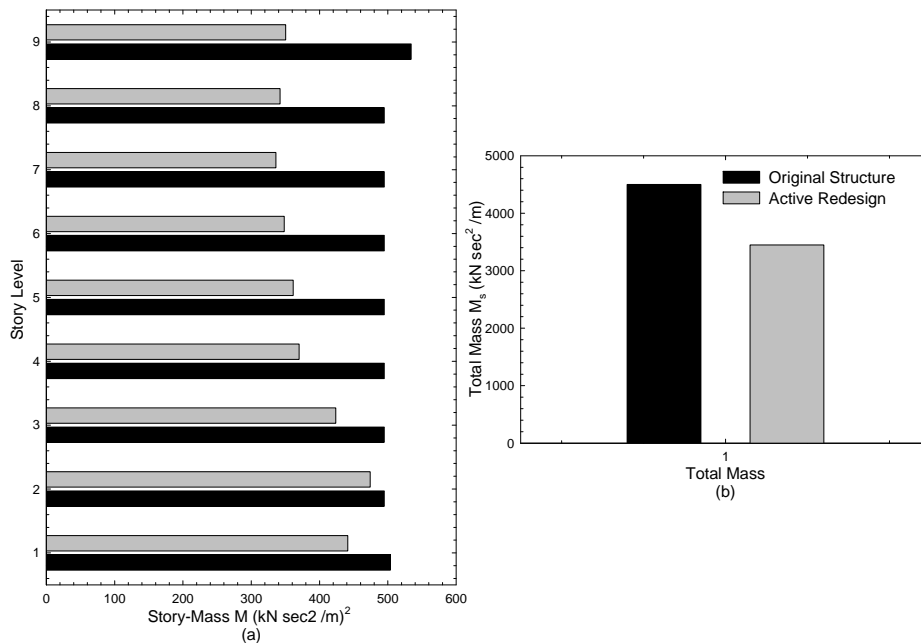


Figure 6 Structural Mass Ms before and after Redesign of the MRF

After the structure and controller are designed independently in *Step 1*, the controller and the building are redesigned together in *Step 2* in order to achieve the same performance (*Target Response*) by reducing the amount of active control power.

The initial total energy transferred to the structure from the controller is equal to 2623.0 N•m•sec and, after redesign, is equal to 1972.1 N•m•sec, so the percentage of reduction of the total energy transferred is 24.81% in *Step 2* of the procedure. Results of the redesign procedure are shown in columns 4, 5 and 6 of Table 4.

Comparisons between the *Target Response* and the *Active Redesign* response are shown in Figure 5. The optimal structural parameters (M , K and C) after active redesign are shown in Table 5. Finally, the story mass distributions before and after redesign are shown in Figure 6a, while the total mass reduction is shown in Figure 6b.

Conclusions

A redesign approach has been outlined in this paper to determine the optimal control/structural system such that an optimal structural configuration can be achieved while satisfying a specified performance objective. It is shown that, using the two-step redesign approach, an efficient solution procedure can be developed. While a one-story one-bay structure and a nine-story shear-type building are used as numerical examples, the redesign approach is equally efficient in dealing with multi-degree-of-freedom nonlinear structural systems.

Acknowledgments

This research was conducted at University at Buffalo and supported by Multi-disciplinary Center for Earthquake Engineering Research (MCEER), which in turn is supported by the Earthquake Engineering Research Centers Program of the National Science Foundation under the Award EEC 970147. Any opinions, findings and conclusions or recommendations expressed in this report are those of the author(s) and do not necessarily reflect those of the Multidisciplinary Center for Earthquake Engineering Research (MCEER), the National Science Foundation (NSF), the State of New York (NYS) or the University at Buffalo.

References

- [1] T. T. Soong and G. D. Manolis. "Active structures." *Journal of Structural Engineering, ASCE*, 113 (1987), p. 2290-2301.
- [2] T. T. Soong. "Active Structural Control: Theory and Practice." *Longman Scientific & Technical*, England (1990).
- [3] M. J. Smith, K. M. Grigoriadis and R. Skelton. "Optimal Mix of Passive and Active Control in Structures." *Journal of Guidance, Control and Dynamics*, Vol. 15(4) (1992), p. 912-919.
- [4] Y. Ohtori, R.E. Christenson, B.F. Spencer and S.J. Dyke. "Benchmark Control Problems for Seismically Excited Nonlinear Buildings." *Journal of Engineering Mechanics, ASCE*, 130(4), (2004), p. 366-385.
- [5] N. Gluck, A. Reinhorn and R. Levy. "Design of supplemental dampers for control of structures." *Journal of Structural Engineering, ASCE*, 122(12), (1996) p. 1394-1399.
- [6] G.P. Cimellaro, T. T. Soong and A. M. Reinhorn. "Optimal integrated design of controlled structures." *Journal of Structural Engineering, ASCE*, (2008) Submitted for publication.